A 3D Voronoi-based Skeleton and Associated Surface Features

Masayuki Hisada [†,§] Alexander G. Belyaev [†] Tosiyasu L. Kunii [‡,§]
masa@hisada.org http://www.u-aizu.ac.jp/∼belyaev/ tosi@kunii.com

[†] The University of Aizu, Aizu-Wakamatsu City, Fukushima 965-8580 Japan

[‡] Hosei University, 3-7-2 Kajino-cho, Koganei City, Tokyo 184-8584 Japan

[§] IT Institute, Kanazawa Institute of Technology, 1-15-13 Jingumae, Shibuya-ku, Tokyo 150-0001, Japan

Abstract

The paper proposes an approach for stable extraction of the skeleton of a polygonal surface and detection of surface features, ridges and ravines, corresponding to skeletal edges. The approach adapts the three-dimensional Voronoi diagram technique [3] for skeleton extraction, explores the singularity theory for ridge and ravine detection [8], and combines several filtering methods for skeleton denoising and for selecting perceptually salient ridges and ravines.

Rather than extract the skeleton as a CW-complex, we approximate it by a two-sided surface. It allows us to use standard mesh editing tools for skeleton denoising and achieve stable extraction of the ridges and ravines.

Keywords: polygonal surface, 3D Voronoi diagram, skeleton, ridges and ravines.

1. Introduction

The skeleton of a 3D surface is the closure of the set of points with more than one closest point on the surface. Mathematically speaking, given an oriented surface, the skeleton is formed by the set of singularities of the signed distance function from the surface [6]. Thus we distinguish two skeletons of an oriented surface, the inner skeleton and the outer skeleton (one of them may be empty, for example, for a surface bounding a convex figure).

In this paper, we develop an approach for stable extraction of the skeleton of a surface approximated by polygonal mesh and detection of surface features (ridges and ravines) corresponding to skeletal edges, see Fig. 1. Our approach adapts the three-dimensional Voronoi diagram technique [3] for skeleton extraction, explores the singularity theory for ridge and ravine detection [8], and combines several filtering methods for skeletal noise reduction and for selecting perceptually salient ridges and ravines.

The skeleton (or medial axis) was originally invented by Blum [13, 12] for 2D shapes and since than has been extensively used for image processing and pattern recognition purposes. The skeleton provides us with symmetry-based shape representation and has been also studied in connection with human shape perception theories [12], [20].

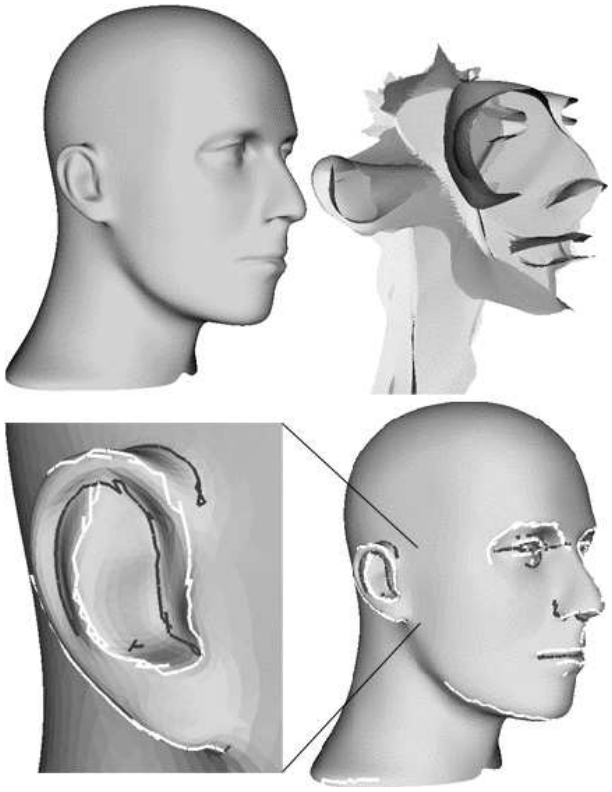

Fig. 1. Mannequin head model, its inner skeleton, and surface features, ridges (white) and ravines (black) corresponding to skeletal edges.

In 3D, the skeleton has been recently studied in connection with a research on shape organization [15], analysis of 3D images [17], and used for shape manipulation purposes [22, 11].

Robust skeletonizing 3D shapes represented by polygonal meshes is a difficult problem because small shape per-

turbations may result in large changes of the skeleton structure. Several algorithms based on the 3D Voronoi diagram were recently proposed [23, 3, 2, 4] (see also references therein). The skeleton was reconstructed as a polygonal CW-complex and many tricks were proposed in order to extract the skeleton topology correctly and achieve computational stability [23, 4].

Our approach for skeleton extraction is also based on the 3D Voronoi diagram. However, in contrast to the previous works, we do not extract the skeleton as a CW-complex. Instead we approximate the skeleton by a two-sided surface. It allows us to use standard mesh editing tools for skeleton denoising.

Mathematically speaking, the skeleton of a surface in 3D is a CW-complex, a geometric figure constructed from curvelinear polygons (cells) by gluing and pasting them together along their edges such that vertices are sewn to vertices and whole edges are sewn to whole edges. The skeleton can be defined as the set of singularities of the distance function from the surface [6]. For a generic surface, the skeleton consists of points whose small neighborhoods on the skeleton are topologically equivalent to a disk (inner skeleton point), a half-disk (skeletal edge point), a disc sewn with a quarter-disk, a disc sewn with a half-disk, and a disc sewn with three quarter-disks [6]. See Fig. 2.

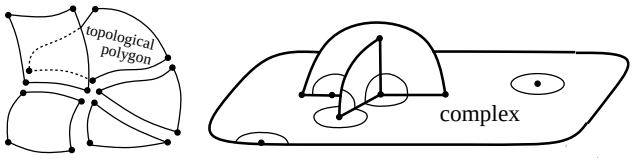

Fig. 2. Singularities of distance function from generic surface for CW-complex which has five types of topologically different points.

The skeletal edges correspond to surface curves, ridges and ravines, at which the surface bends sharply [6], see Fig. 3. The ridges and ravines form a subset of the extrema of the principal curvatures along their principal directions [25, 5, 8]

The ridges and ravines are important surface descriptors. Detection of them is difficult because of their non-local nature. Several methods were proposed for detection of their local counterparts defined via curvature extrema on surfaces approximated by triangle meshes [19, 9, 24]. However curvature extrema detection is not a simple task because it involves estimation of high-order surface derivatives and work is in progress to achieve stable detection of curvature extrema surface features [21]. So there is a need in a simple and reliable method for stable detection of ridges and ravines on polygonal surfaces.

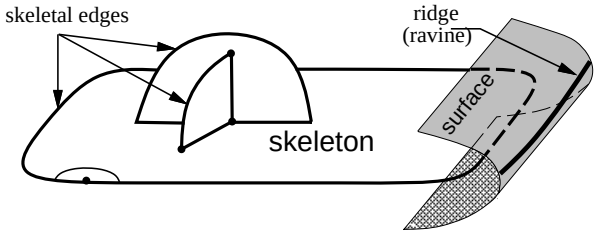

Fig. 3. It is natural to define ridges and ravines as surface curves corresponding to skeletal edges.

In this paper, we propose such a method. After extracting the skeleton (skeletal surface) we use the Laplacian smoothing scheme for skeleton denoising and a statistical analysis of the skeletal edges for selecting perceptually salient ridges and ravines.

2. Voronoi Vertices and Skeleton

Given a set of points called sites in nD space, the Voronoi diagram of the set is a partition of the space into regions (Voronoi regions), each of which consists of the space points closer to one particular site than to any other site. Each Voronoi region is a convex polytope, and its vertices are called Voronoi vertices. Each Voronoi vertex is equidistant from $n+1$ or more original points. Let us recall that the skeleton of a hypersurface in nD is the closure of the set of points with more than one closest point on the hypersurface.

Thus we can expect that if the original points are uniformly and densely distributed along a given hypersurface, the Voronoi vertices will provide a good approximation of the skeleton. It turns out to be true in $2D$, see Fig. 4 for a set of points uniformly distributed along a $2D$ curve and associated Voronoi diagram. However in nD, only a subset of the Voronoi vertices approximate the skeleton [3, 2].

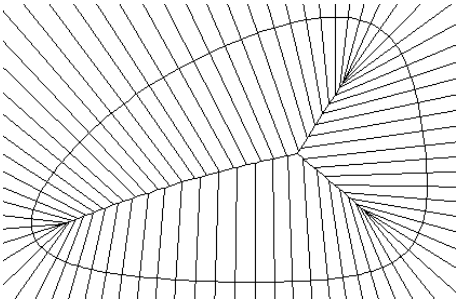

Fig. 4. Voronoi diagram of set of points uniformly distributed along curve.

The left image of Fig. 5 depicts a set of points distributed uniformly along an ellipsoid and the Voronoi vertices of the set. The skeleton of an ellipsoid consists of an ellipse and its inner part located inside the ellipsoid. Thus many Voronoi vertices are not located near the skeleton.

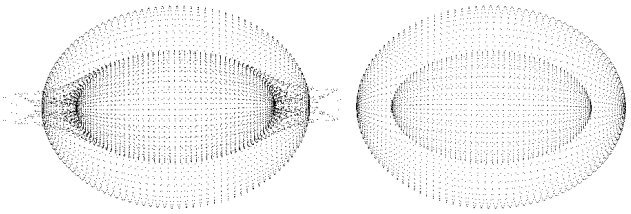

Fig. 5. Left: Points uniformly distributed along ellipsoid and associated Voronoi vertices. Right: Points uniformly distributed along ellipsoid and Voronoi poles.

A simple procedure for selecting proper Voronoi vertices of a given set of points distributed along a surface was proposed in [3]. For each point let us consider its associated Voronoi region and select the Voronoi poles, two vertices of the region farthest from the point, one on either side. It turns out that the poles are located near the skeleton of the surface. Moreover if the initial set of points is dense enough the poles provide a good approximation of the skeleton [3] (for a rigorous mathematical study see [2]).

The right image of Fig. 5 shows the Voronoi poles associated with a set of points uniformly distributed along an ellipsoid. Note how good the poles approximate the skeleton.

The skeleton of a closed surface consists of two parts. Consequently, the Voronoi poles form two clouds of points. Fig. 6 shows the clouds of points formed by the inner and outer Voronoi poles for the Cyberware Venus head model.

3. Skeleton Reconstruction from Voronoi Poles

We now want to reconstruct the skeleton from the set of Voronoi poles. Unfortunately popular computational geometry algorithms for shape reconstruction from a cloud of points [3, 10, 7, 1] do not provide us with a reliable reconstruction of the skeleton because of its CW-complex nature. For example, Fig. 7 presents reconstruction of the inner skeleton of the Mannequin head model by the Crust algorithm. The algorithm fails to reconstruct the skeleton properly near non-manifold points. The anti-crust algorithm developed for 2D skeleton reconstruction [16] (see also references therein) also produces poor results in 3D. Moreover fairing of the skeleton given as a CW-complex would be a complex procedure [18].

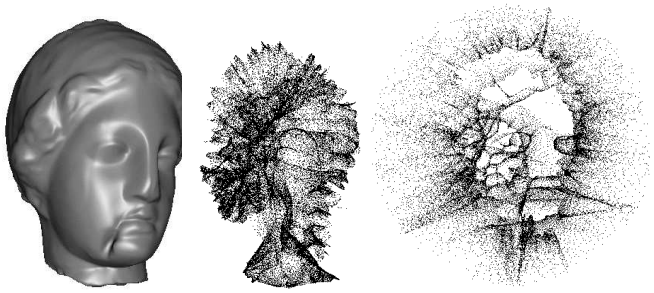

Fig. 6. Cyberware Venus head model and clouds of points formed by inner and outer Voronoi poles (different scales are used).

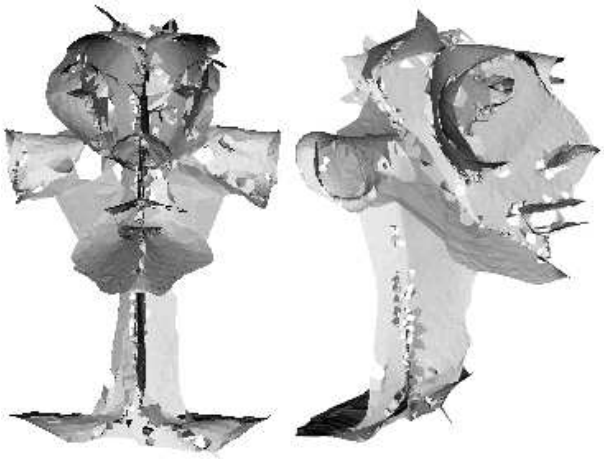

Fig. 7. Reconstruction of inner skeleton of Mannequin head model by Crust algorithm. Note many holes near non-manifold skeleton points.

All this motivates us to give up with CW-complex skeleton representation and instead to reconstruct the skeleton as a two-sided surface (with possible self-intersections). Our idea is extremely simple. Given a surface approximated by a triangle mesh, two Voronoi poles are connected by an edge if and only if their corresponding mesh vertices are connected by a mesh edge, see Fig. 8. So each mesh triangle corresponds to a triangle made by associated Voronoi poles.

Fig. 9 shows the inner skeleton of the Mannequin head model. The skeleton is reconstructed as a two-sided surface.

A good approximation of the skeleton by the Voronoi poles is achieved when the original mesh is dense enough. So for sparse meshes we use several rounds of the Loop subdivision in order to obtain a sufficiently dense mesh. Fig. 10 demonstrates how the skeleton reconstruction quality de-

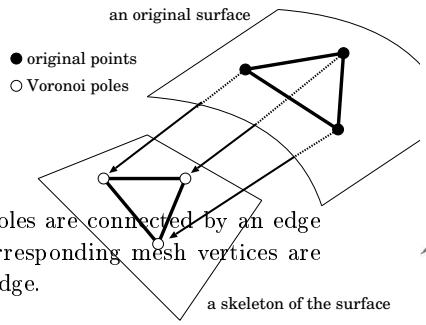

Fig. 8. Two Voronoi poles are connected by an edge if and only if their corresponding mesh vertices are connected by a mesh edge.

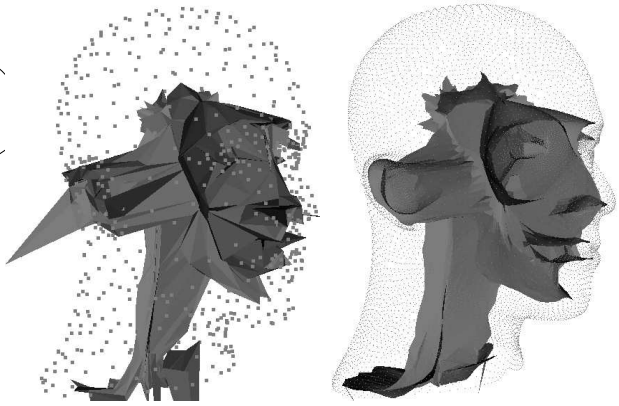

Fig. 10. Left: Original mannequin head point dataset (689 points) and inner skeleton reconstructed from Voronoi poles. Right: mannequin head point dataset after two Loop subdivisions (10,883 points) and inner skeleton.

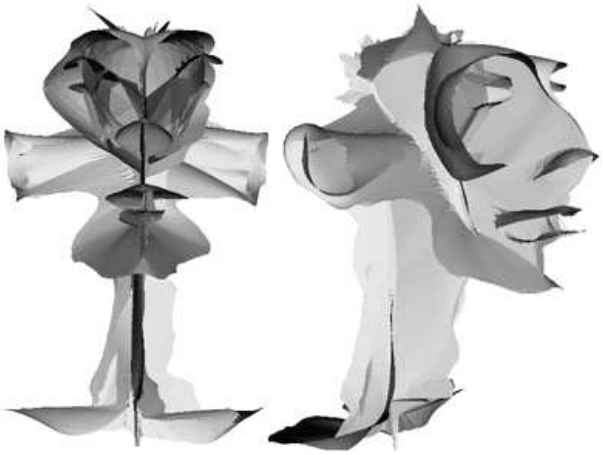

Fig. 9. Mannequin head inner skeleton reconstructed from Voronoi poles as two-sided surface.

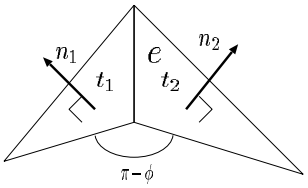

Fig. 11. Edge e is sharp if $\boldsymbol{n}_1 \cdot \boldsymbol{n}_2$ is close to -1 where $\boldsymbol{n}_1$ and $\boldsymbol{n}_2$ are orientation normals of two adjacent triangles t_1 and t_2 sharing e.

pends on the mesh density of the original surface.

4. Detection of Ridges and Ravines

Given a surface and its skeleton, we want to detect surface features, ridges and ravines, corresponding to the skeletal edges, as seen in Fig. 3. Since we reconstructed the skeleton as a two-sided polygonal surface (skeletal surface), the ridges and ravines correspond to sharp edges of the skeletal surface.

Let t_1 and t_2 be triangles of the skeletal surface sharing a common edge e. We orient the skeletal surface by the unit normal directed toward the original surface. Let $\boldsymbol{n}_1$ and $\boldsymbol{n}_2$ be the orientation normals at t_1 and t_2, respectively. See Fig. 11.

We consider e as a sharp edge if ϕ, the angle between the normals, satisfies

$$-1 \leq \cos\phi = \boldsymbol{n}_1 \cdot \boldsymbol{n}_2 \leq T,$$

where T is a threshold.

We use a statistical approach in order to choose T. Consider the histogram of $\cos\phi$ over all the inner edges of the skeletal surface. For example, Fig. 12 presents the histogram corresponding to the inner skeletal surface of the mannequin head model. As expected, the skeletal surface mostly consists of flat parts connected by sharp edges. Let us define the threshold T analysing the histogram of $\cos\phi$. For example, one can choose T such that for 3 percent of edges $-1 \leq \cos\phi < T$. Fig. 13 visualizes only those edges of the inner skeleton of the mannequin head model for which $-1 \leq \cos\phi < T_{3\%}$.

In order to improve the connectivity between sharp edges we use a hysteresis thresholding idea introduced in [14]. We choose two thresholds $T_{3\%}$ and $T_{5\%}$ at the 3rd and 5th percentiles of the edge-sharpness data for the entire skeletal surface, i.e., $T_{5\%}$ is chosen so that for 5 percent of edges $\cos\phi$ is below that value. Let us call the edges satisfying $\cos\phi < T_{3\%}$ the strong sharp edges and the edges satisfying $\cos\phi < T_{5\%}$ the weak sharp edges. We keep a con-

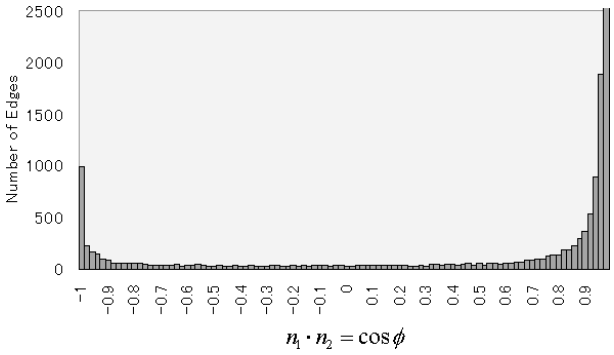

Fig. 12. Histogram of $\cos\phi$ for inner skeleton of mannequin head model.

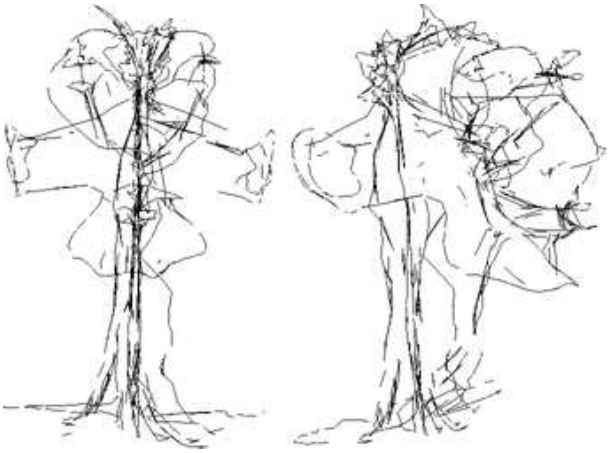

Fig. 13. 3% edges from left side of histogram of $cos\phi$.

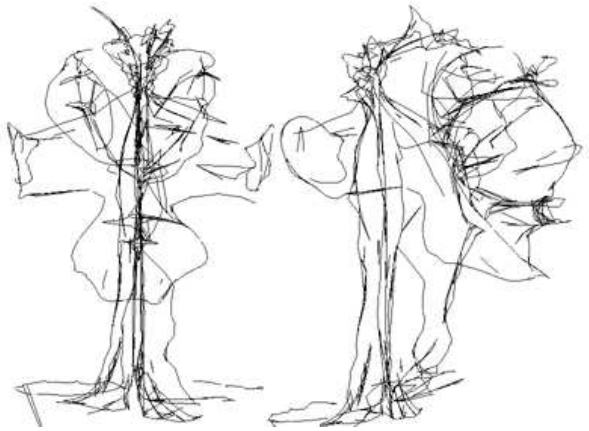

Fig. 14. Hysteresis thresholding with $T_{3\%}$ and $T_{5\%}$ is used to achieve better connectivity of sharp edges.

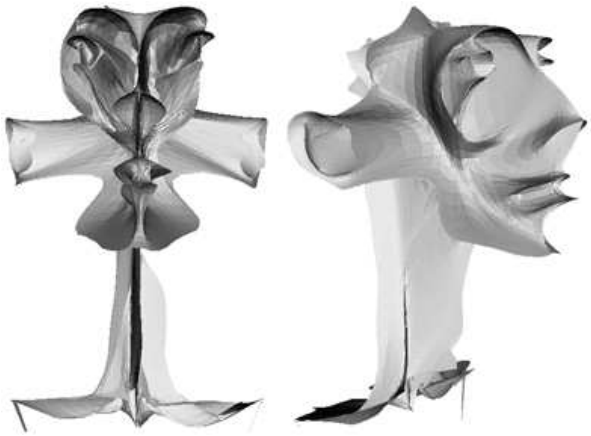

Fig. 15. Mannequin head inner skeleton smoothed by Laplacian smoothing flow.

nected chain of weak sharp edges only if the chain contains at least one strong sharp edge. Fig. 14 demonstrates how the hysteresis thresholding improves the connectivity of sharp edges.

Since the skeleton is very sensitive to small perturbations of the geometry of the original surface, we smooth the skeletal surface by the Laplacian smoothing flow which repeatedly and simultaneously moves each mesh vertex by a displacement equal to a positive scale factor times the difference between the average of the neighboring vertices and the vertex itself.

Laplacian smoothing improves the appearance of the skeletal surface, as seen in Fig. 15.

Unfortunately Laplacian smoothing destroys sharp edges of the skeletal surface, as seen in Fig. 16. So we have to strengthen the hysteresis thresholding conditions, see Fig. 17.

In order to achieve stable detection of perceptually salient ridges and ravines we use also another filtering procedure based on a simple statistical analysis of the distances between the vertices of sharp edges and their corresponding vertices on the original surface. Local curvature analysis [5, 9] shows that the most salient ridges and ravines of the surface correspond to skeletal edges closest to the surface. So we specify a threshold T_{dist} and keep only those vertices of sharp skeletal edges, for which the distance is below T_{dist}. We compute T_{dist} independently for the inner and outer skeletons. To choose T_{dist} for the inner skeleton, we construct the histogram of the distances computed for the vertices of the edges of the inner skeleton and select T_{dist} such that 40% percent of distance is below T_{dist}. Fig. 18 demonstrate advantages of this simple distance filtering scheme.

Although we demonstrated our technique using a simple mannequin head model, it works well for much more

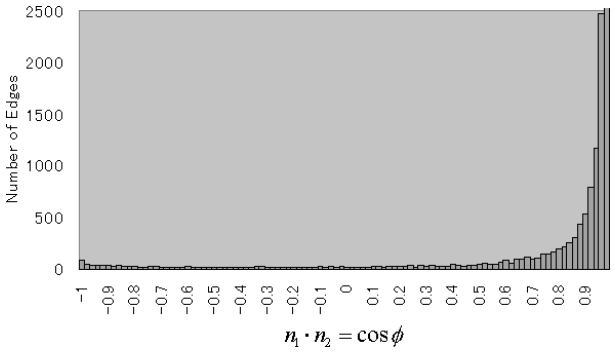

Fig. 16. Histogram of $\cos\phi$ for inner skeleton of mannequin head model smoothed by Laplacian smoothing flow.

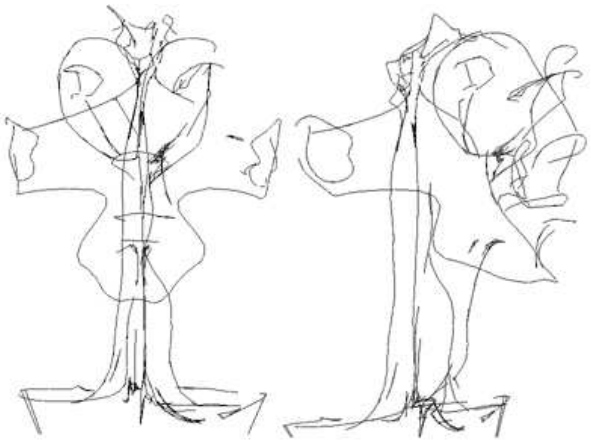

Fig. 17. Hysteresis thresholding with $T_{1\%}$ and $T_{3\%}$ is used to detect sharp edges of smoothed inner skeleton of mannequin head model.

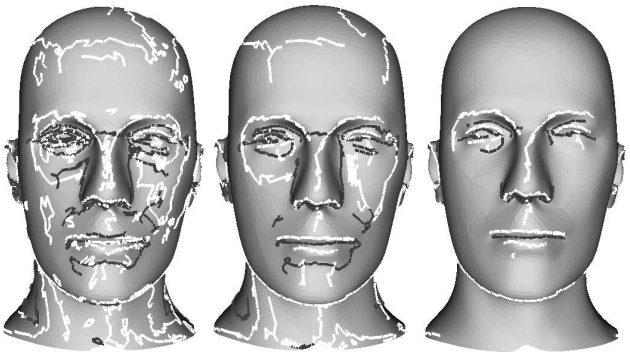

Fig. 18. Ridges (white) and ravines (black) detected on mannequin head model after hysteresis thresholding was applied to select sharp skeletal edges. Left: no surface smoothing was done. Middle: Laplacian smoothing was applied. Right: Laplacian smoothing and distance-based filtering were used; 40% distance threshold is used for inner skeletal edges and 50% distance threshold is used for outer skeletal edges.

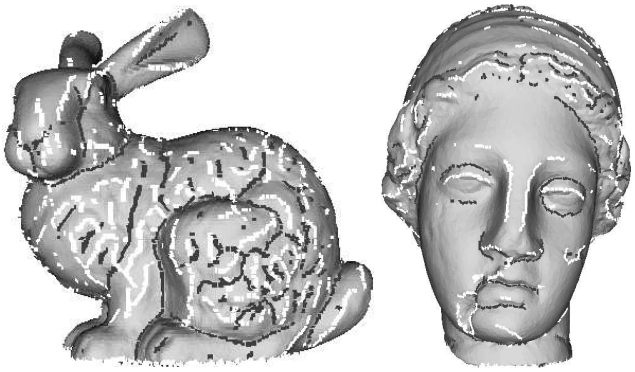

Fig. 19. Salient ridges (white) and ravines (black) detected on complex polygonal models.

complex meshes. Fig. 19 shows ridges and ravines detected on the Stanford bunny model and Cyberware Venus head model.

5. Conclusion

We proposed an approach for stable extraction of the skeleton of a surface approximated by polygonal mesh and detection salient ridges and ravines. Our method for skeleton extraction is based on the 3D Voronoi diagram. However, in contrast to the previous works, we do not extract the skeleton as a CW-complex. Instead we approximate the skeleton by a two-sided surface. It allows us to use standard mesh editing tools for skeleton denoising. We also apply statistical filtering methods for selecting perceptually salient ridges and ravines.

References

[1] U. Adamy, J. Giesen, and M. John. New techniques for topologically correct surface reconstruction. In *Proceedings of IEEE Visualization 2000*, pages 373–380, October 2000.

[2] N. Amenta and M. Bern. Surface reconstruction by Voronoi filtering. *Discrete and Computational Geometry*, 22:481–504, 1999.

[3] N. Amenta, M. Bern, and M. Kamvysselis. A new Voronoi-based surface reconstruction algorithm. *Computer Graphics (Proceedings of SIGGRAPH 98)*, pages 415–421, 1998.

[4] N. Amenta, S. Choi, and R. Kolluri. The power crust. In *Proceedings of 6th ACM Symposium on Solid Modeling*, pages 249–260, 2001.

[5] E. V. Anoshkina, A. G. Belyaev, and T. L. Kunii. Detection of ridges and ravines based on caustic singularities. *International Journal for Shape Modeling*, 1(1):13–22, 1994.

[6] E. V. Anoshkina, A. G. Belyaev, O. G. Okunev, and T. L. Kunii. Ridges and ravines: a singularity approach. *International Journal for Shape Modeling*, 1(1):1–11, 1994.

[7] M. Attene and M. Spagnuolo. Automatic surface reconstruction from point sets in space. *Computer Graphics Forum (Eurographics 2000)*, 19(3):457–465, 2000.

[8] A. G. Belyaev, E. V. Anoshkina, and T. L. Kunii. Ridges, ravines, and singularities. In A. T. Fomenko, and T. L. Kunii, *Topological Modeling for Visualization*. Ch. 18, pages 375–383, Springer, 1997.

[9] A. G. Belyaev and Y. Ohtake. An image processing approach to detection of ridges and ravines on polygonal surfaces. In A. de Sousa and J. C. Torres, editors, *Eurographics 2000, Short Presentations*, pages 19–28, August 2000.

[10] F. Bernardini, J. Mittleman, H. Rushmeier, C. Silva, and G. Taubin. The ball-pivoting algorithm for surface reconstruction. *IEEE Transactions on Visualization and Computer Graphics*, 5(4):349–359, 1999.

[11] J. Bloomenthal and C. Lim. Skeletal methods of shape manipulation. In *Proceedings of International Conference on Shape Modeling and Applications*, pages 44–47, Aizu-Wakamatsu, Japan, March 1999.

[12] H. Blum. A transformation for extracting new descriptors of shape. In W. Wathen-Dunn, editor, *Symposium on Models for the Perception of Speech and Visual Form*, pages 362–380. MIT Press, 1967.

[13] H. Blum. Biological shape and visual science. *J. Theor. Biology*, 38:205–287, 1973.

[14] J. Canny. A computational approach to edge detection. *IEEE Transactions on Pattern Analysis and Machine Intelligence*, 8(6):679–698, 1986.

[15] P. Giblin and B. B. Kimia. A formal classification of 3D medial axis points and their local geometry. In *Computer Vision and Pattern Recognition (CVPR'00), Vol. I*, pages 566–575, 2000.

[16] C. Gold. Crust and anti-crust: a one-step boundary and skeleton extraction algorithm. In *Proc. 15th Symp. Computational Geometry*, pages 189–196. ACM, 1999.

[17] J. Gomes and O. Faugeras. Reconciling distance functions and level sets. *Journal of Visual Communication and Image Representation*, 11(2):209–223, June 2000.

[18] A. Hubeli and M. Gross. Fairing of non-manifolds for visualization. In *Proceedings of IEEE Visualization 2000*, pages 407–414, October 2000.

[19] G. Lukács and L. Andor. Computing natural division lines on free-form surfaces based on measured data. In M. Dæhlen, T. Lyche, and L. L. Schumaker, editors, *Mathematical Methods for Curves and Surfaces II*, pages 319–326. Vanderbilt Univ. Press, 1998.

[20] D. Mumford. Mathematical theories of shape: Do they model perception. In B. C. Vemuri, editor, *Geometric Methods in Computer Vision, Proc. SPIE 1570*, 1991.

[21] Y. Ohtake, M. Horikawa, and A. G. Belyaev. Adaptive smoothing tangential direction fields on polygonal surfaces. Pacific Graphics 2001, Tokyo, October 2001.

[22] D. W. Storti, G. M. Turkiyyah, M. A. Ganter, C. Lim, and D. M. Stat. Skeleton-based modeling operations on solids. In *SMA '97: Proceedings of the Fourth Symposium on Solid Modeling and Applications*, pages 141–154, Atlanta, May 1997.

[23] G. M. Turkiyyah, D. W. Storti, M. Ganter, H. Chen, and M. Vimawala. An accelerated triangulation method for computing the skeletons of free-form solid models. *Computer-Aided Design*, 29(1):5–19, 1997.

[24] K. Watanabe and A. G. Belyaev. Detection of salient curvature features on polygonal surfaces. *Computer Graphics Forum (Eurographics 2001 issue)*, 20(3):385–392, 2001.

[25] A. Yuille and M. Leyton. 3D symmetry-curvature duality theorems. *Graphical Models and Image Processing*, 52(1):124–140, 1990.